Published in final edited form as:
Brain Res. 2011 July 11; 1400: 42–52. doi:10.1016/j.brainres.2011.05.036.

The adaptive pattern of the auditory N1 peak revealed by standardized low-resolution brain electromagnetic tomography

Fawen Zhang[*], **Aniruddha Deshpande**[*], **Chelsea Benson**[*], **Mathew Smith**[±], **James Eliassen**[±], and **Qian-Jie Fu**[®]

[*]Department of Communication Sciences and Disorders, University of Cincinnati OH, USA

[±]Center for Imaging Research, University of Cincinnati OH, USA

[®]House Ear Institute, Los Angeles, CA, USA

Abstract

The N1 peak in the late auditory evoked potential (LAEP) decreases in amplitude following stimulus repetition, displaying an adaptive pattern. The present study explored the functional neural substrates that may underlie the N1 adaptive pattern using standardized Low Resolution Electromagnetic Tomography (sLORETA). Fourteen young normal hearing (NH) listeners participated in the study. Tone bursts (80 dB SPL) were binaurally presented via insert earphones in trains of ten; the inter-stimulus interval was 0.7 s and the inter-train interval was 15 s. Current source density analysis was performed for the N1 evoked by the 1st, 2nd and 10th stimuli (S_1, S_2 and S_{10}) at three different timeframes that corresponded to the latency ranges of the N1 waveform subcomponents (70–100, 100–130 and 130–160 ms). The data showed that S_1 activated broad regions in different cortical lobes and the activation was much smaller for S_2 and S_{10}. Response differences in the LAEP waveform and sLORETA were observed between S_1 and S_2, but not between the S_2 and S_{10}. The sLORETA comparison map between S_1 and S_2 response showed the activation was located in the parietal lobe for the 70–100 ms timeframe, the frontal and limbic lobes for the 100–130 ms timeframe, and the frontal lobe for the 130–160 ms timeframe. These sLORETA comparison results suggest a parieto-frontal network that might help to sensitize the brain to novel stimuli by filtering out repetitive and irrelevant stimuli. This study demonstrates that sLORETA may be useful for identifying generators of scalp-recorded event related potentials and for examining the physiological features of these generators. This technique could be especially useful for cortical source localization in individuals who cannot be examined with functional magnetic resonance imaging or magnetoencephalography (e.g., cochlear implant users).

Keywords

Auditory cortex; Auditory evoked response; Electrophysiology; Adaptation; Human

Corresponding author: Fawen Zhang, Department of Communication Sciences and Disorders, University of Cincinnati, 3202 Eden Ave., Cincinnati, OH, USA 45267-0379, Phone: 513-558-8513, Fax : 513-558-8500, Fawen.Zhang@uc.edu.

1. Introduction

The human auditory system displays a decrease in neural responsiveness following stimulus repetition, due to the adaptation and refractory features of neurons. Neural adaptation is a process in which neural responses are continuously recalibrated according to incoming stimuli (Budd et al., 1998). Adaptation may be reflected by decreased responsiveness of neurons following stimulus repetition. Neural adaptation has been suggested to reduce the sensitivity of the auditory system to repeated stimuli and enhances the sensitivity to novel stimuli (Delgutte, 1997). Neural refractoriness is the phenomenon wherein a neuron can only respond to a stimulus after a sufficient period of recovery following a response to a preceding stimulus (Shore, 1995; Fitzpatrick et al., 1999). Refractoriness has been suggested to be related to the limitation of the temporal coding ability of neurons (Shore, 1995; Fitzpatrick et al., 1999).

The late auditory evoked potential (LAEP) is a type of event related potential (ERP) that can be recorded from the scalp using electroencephalographic (EEG) techniques. The LAEP reflects neural activity occurring 50–250 ms after the presentation of an auditory stimulus (Näätänen & Picton, 1987; Pool et al., 1989; Eggermont & Ponton, 2002; Martin et al., 2008). Among the several peaks of the LAEP, the N1 is the most frequently studied component. The N1 consists of several subcomponents based on the waveform latency and scalp current distribution. The N1a subcomponent, at approximately 75 ms, is most prominent at temporal electrodes. The N1b subcomponent, at about 100 ms, is most prominent at vertex electrodes. The N1c subcomponent, at about 130 ms, is most prominent at temporal electrodes but extends to fronto-polar and lateral central electrodes (Knight et al., 1988; Woods, 1995). Extensive evidence from previous studies suggests that distinctions between N1 subcomponents should be made in terms of neural generators (sources) rather than the latency and scalp current distribution, as the cerebral generators contributing to the N1 appear to be spatially and temporally overlapping (e.g., Budd et al., 1998).

The amplitude decrement of the N1 following repeated stimuli has been studied using a stimulus-train paradigm (Fruhstorfer, 1971; Prosser et al., 1981; Bourbon et al., 1987; Barry et al., 1992; Budd et al., 1998). Because the adaptation and refractory processes in the response cannot be simply separated, we will use the term “the N1 adaptive pattern” throughout the paper to indicate the N1 amplitude reduction following stimulus repetition. Most previous studies typically treated the N1 as a unitary peak and reported that, with an inter-stimulus interval (ISI) of approximately 1 s, the N1 amplitude is reduced by approximately 50–70% over the first two or three stimuli before reaching an asymptotic level (Ritter et al., 1968; Bourbon et al., 1987). The amplitude reduction following stimulus repetition is not obvious when the ISI is greater than 10 s (Ritter et al., 1968; Näätänen & Picton, 1987; Alcaini et al., 1994; Zhang et al., 2009b).

While there is some understanding of brain structures for the generation of the N1, it is unclear which neuroanatomical and functional substrates contribute to the N1 adaptive pattern. This prevents effective diagnosis and treatment of patients whose auditory pathology leads to an abnormal neural adaptive pattern. For example, in cochlear implant (CI) users, long term deafness can alter adaptation and refractory features of neurons (Westerman & Smith, 1984; Loquet et al., 2004). Recently there has been increased interest in using neurologic and audiologic applications of the LAEP to predict CI patient outcomes, as well as to document brain plasticity following implantation (Groenen et al., 2001; Ponton el al., 1996; Hine & Debener, 2007; Guiraud et al., 2007; Zhang et al., 2010). Better understanding of the neural mechanisms that may underlie the N1 adaptive pattern will provide more effective electrophysiological tools with which to objectively measure brain function and plasticity in these patients.

The EEG data recorded at various scalp locations can be used to estimate the current source generators in the brain by advanced signal processing techniques. The source analysis would provide important neuroanatomical and functional information of brain regions contributing to the EEG data, with excellent temporal resolution. However, it is impossible to reconstruct a unique intracranial electrical source in the human brain with the given EEG signals (referred to as "inverse problem"), as some sources produce electrical signals that cancel each other out. Among many source analysis techniques, the sLORETA (standardized Low Resolution Brain Electromagnetic Tomography) method provides an excellent solution to the inverse problem, even in the presence of measurement and biological noise (Pascual-Marqui, 2002; Wagner et al., 2004; Grech et al., 2008). With sLORETA, estimations of EEG sources are computed within a 3-shell spherical head model registered to the Talairach human brain atlas. This produces 6239 voxels at 5 mm resolution in the cortical gray matter and hippocampus areas. The maps are derived based on a location-wise inverse weighting of the results of a minimum norm least squares (MNLS) analysis with their estimated variances. Therefore, it does not require assumptions about the number, localization, or configuration of neuronal sources (Pascual-Marqui, 2002). Because the assumption of sLORETA is that coherent and synchronized co-activation of neighboring cortical regions is needed to generate EEG signals, the sLORETA provides a "blurred-localized" image of a source that conserves the location of maximal activity. Despite the blurred image, sLORETA had zero error location when reconstructing single sources, that is, the maximum of the current density power estimate coincides with the exact dipole location.

The specific aim of this paper was to estimate the electric sources or neural generators contributing to the scalp-recorded auditory N1 and its adaptive pattern using sLORETA in NH listeners. This will set the stage for further studies of the N1 adaptive pattern in CI patients. Moreover, the results will deepen our understanding of the neural mechanisms underlying the brain functions related to normal and abnormal N1 adaptive pattern.

2. Results

2.1. Scalp ERPs

Figure 1 illustrates the grand-average LAEPs across subjects at selected scalp sites for S_1, S_2, and S_{10} in the train. The topography of the 40-channel map is also shown on the right upper corner of the figure. Responses were the largest at Cz with the N1 latency at approximately 100 ms and P2 latency at 200 ms. The responses became smaller at electrodes that were further away from Cz. The response was greatly reduced for S_2 than for S_1. The difference between the S_2 response and the S_{10} response was small. In addition to the peak amplitude differences in the LAEP between S_1 and later stimuli, there were some morphological differences. An additional peak occurring at approximately 300 ms after stimulus onset was observed for S_1, but not for later stimuli.

Figure 2 shows the mean N1 amplitudes and latencies for S_1, S_2, and S_{10}. The mean N1 latencies for S_1, S_2, and S_{10} were 113.18 ms, 98.71 ms and 96.99 ms, respectively. A one-way RM ANOVA showed that there was a significant stimulus order effect on the N1 latency ($F_{(2,12)} = 12.00$, $p < 0.05$). Post-hoc Bonferroni pairwise comparisons showed that the N1 latency for S_1 was significantly longer than for S_2 ($p < 0.05$) or S_{10} ($p < 0.05$); there was no significant difference between the S_2 and S_{10} responses ($p = 0.37$). The mean N1 amplitudes for S_1, S_2 and S_{10} were −10.04 μV, −3.64 μV and −3.0 μV, respectively. There was a significant stimulus order effect on N1 amplitude ($F_{(2,12)} = 23.46$, $p < 0.05$). Post-hoc comparisons showed that the N1 amplitude for S_1 was significantly larger than that for S_2 ($p < 0.05$) or S_{10} ($p < 0.05$); Again, there was no significant difference between the S_2 and S_{10} response amplitudes ($p = 0.32$).

2.2. sLORETA

The statistical analysis was performed on the activity between each of the 3 timeframes (70–100 ms, 100–130 ms, and 130–160 ms) and the pre-stimulus period. Figure 3 shows images of average CSD distributions for S_1, S_2, and S_{10} at the time points corresponding to the maximum sLORETA values within the 3 timeframes (70–100 ms, 100–130 ms, and 130–160 ms). We display the results at the time points corresponding to the maximum sLORETA activation instead of the results of averaged sLORETA values over those timeframes because: 1) The former approach has been used in previous studies (Knott et al., 2009), and 2) the differences in sLORETA activation between timeframes would be reduced if the average values are used. There was extensive activation for S_1 within each of the timeframes, not only in the temporal lobe but also in other lobes. The activation was largely reduced for S_2. For S_{10}, the activation was more restricted to the temporal lobe in 70–100 ms and 100–130 ms timeframes, but involved non-temporal lobe regions (the frontal lobe and the parietal lobe) in the 130–160 ms timeframe.

Table 1 lists significant activation of structures at the time point corresponding to the maximum sLORETA activation within the three timeframes for S_1, S_2 and S_{10}. Structures consisting of at least 5 activated voxels are included. The data showed that multiple areas in the limbic lobe, temporal lobe, frontal lobe, parietal lobe, occipital lobe, and sub-lobar region were activated within all three timeframes in response to S_1. The activation in response to S_2 was much less than for S_1, in terms of voxel number for the 70–100 ms and 100–130 ms timeframes and in terms of voxel number and the number of involved structures for the 130–160 ms timeframe. The activation in response to S_{10} mainly involved the temporal lobe within the 70–100 ms and 100–130 ms timeframes; the activation shifted to the parietal and frontal lobes for the 130–160 ms timeframe.

The sLORETA difference map between S_1 and S_2 revealed significant decrements in cortical activation, as shown in Figure 4. The time point corresponding to the maximum sLORETA activation for the timeframes of 70–100 ms, 100–130 ms, and 130–160 ms was selected to show the statistical imaging. It was noted that the activation was in the parietal lobe for the 70–100 ms timeframe, the frontal lobe and limbic lobe for the 100–130 ms timeframe, and the frontal lobe for the 130–160 ms timeframe. The specific brain regions are listed in Table 2. In contrast, the sLORETA difference map between S_2 and S_{10} did not yield any significant differences for any of the 3 timeframes.

3. Discussion

This study is the first to examine the neuronal substrates underlying N1 adaptive pattern using a time-course analysis. It provided evidence that multiple brain lobes contribute to the N1, with increasing contribution of the non-specific regions (ie., non-auditory cortex) when the response is evoked by the first stimulus in the train. Moreover, there is a parieto-frontal brain network involved in N1 adaptive pattern.

3.1. Scalp ERPs

Consistent with previous studies (Woods & Elmasian, 1986; Bourbon et al., 1987; Budd et al., 1998), this study found that the N1 amplitude decreased approximately 60% for S_2, after which amplitude values reach an asymptote. In addition to the amplitude difference between LAEPs evoked by S_1 and later stimuli, there were some differences in morphology. The positive peak occurring at 300 ms was obvious for S_1 but not for later stimuli. This peak may be P3 and possibly associated with subjects' expectation of stimuli during the long ITI (Hari et al., 1979). Previous studies also reported that the P3 could be elicited by an unpredictable shift in repetitive stimulus-trains even when subjects were instructed to ignore

stimuli or read a book (Ritter et al., 1968; Squires et al., 1975). This component of P3 reflects the “mismatch” to an ongoing stimulus train and indexes an involuntary attention switch to novel stimuli (Squires et al., 1975; Näätänen & Picton, 1987).

3.2. Generators of the N1 and their adaptive features

Previous studies have reported multiple generators for the N1 (Vaughan & Ritter, 1970; Kooi et al., 1971). Scherg and Cramon (1985) performed dipole analysis on the LAEP data and concluded that the N1 response could be explained by at least 2 major dipole sources: a vertically oriented dipole situated in the primary auditory cortex in the posterior superior temporal plane, and a radially oriented neuronal dipole source located in the auditory association cortex at the superior temporal gyrus (Scherg & Cramon, 1985). The contribution of regions outside of the auditory cortex and association areas are also reported (Woods et al., 1987; Pool et al., 1989; Knight et al., 1988). For instance, patients with lesions of the temporal-parietal junction or the inferior parietal lobe displayed a significant reduction of N1 compared to control subjects (Knight et al., 1988; Woods et al., 1987). A number of ERP, functional magnetic resonant imaging (fMRI), and intracranial recording studies have suggested recruitment of non-auditory (non-specific) regions such as the cingulate cortex in the limbic lobe and structures in the frontal lobe for the N1 peak (Anderer et al., 1998; Picton et al., 1999; Gallinat et al., 2002; Giard et al., 1994; Rosburg et al., 2005). Evidence has also shown that the extralemniscal pathways of the bulbar reticular formation and the centrum medianum of the thalamus may contribute to the N1 (Fruhstorfer, 1971).

One important factor influencing the contributing structures to the N1 across studies is the ISI, which affects neural adaptation and refractoriness. When the ISI is short (e.g., approximately 1 s), the dominant contributor of the N1 is the temporal lobe (Hari et al., 1982; Anderer et al., 1998; Picton et al., 1999). When the ISI is increased, sources in brain regions other than auditory cortex become more active (Hari et al., 1982; Näätänen & Picton, 1987). Using both MEG and EEG techniques, Hari et al. (1982) recorded the LAEP using 1 kHz tone bursts presented with randomized ISIs of 1, 2, 4, 8, 16 s. The authors found that for short ISIs (ie., < 4 s), a wide auditory area in the temporal lobe was activated, extending from the supratemporal plane and the superior temporal gyrus to the parietal operculum and to the inferior parietal lobule. For long ISIs (ie., > 4 s), areas in the frontal cortex, hippocampus and the brainstem nuclei were also activated. Several studies have suggested that it is possible to differentiate N1 components by varying the ISI (Järvilehto et al., 1978; Hari et al., 1979). Alcaini et al. (1994) examined the scalp current density of the LAEP in response to stimuli with various ISIs from 1 to 16 s. The authors reported that two different components contributed to the N1. The first component was elicited with all ISIs, peaking at about 95 ms and exhibiting full recovery below 8 s. The second component was elicited by infrequent stimuli, peaking at approximately 140 ms and exhibiting full recovery above 16 s. Similar results have been reported in other studies (Lu et al., 1992; McEvoy et al., 1997).

The amplitude decrement of the N1 following stimulus repetition, or the N1 adaptive pattern, has been reported and has been largely attributed to neural adaptation. This is because the N1 adaptive pattern meets at least some of adaptation criteria such as: 1) response decrement to repeated stimulation; and 2) direct relation between stimulus repetition rates and response decrement (Thompson and Spencer, 1966). However, neural adaptation is not the only involved mechanism because the N1 adaptive pattern is not an exponential decay (Thompson and Spencer, 1966). Researchers suggested that another important mechanism underlying the N1 adaptive pattern in refractoriness, in which the neurons require a recovery time before they are capable of responding normally to the next signal following the preceding response (Barry et al., 1992; Budd et al., 1998).

The sLORETA results in this study suggest that both adaptation and refractoriness processes have attributed to the N1 adaptive pattern. For instance, some brain activity elicited by S_1 was reduced in the S_2 response and further reduced in the S_{10} response, showing adaptation (see brain activity in the timeframes of 70–100 ms and 100–130 ms, Table 1). In contrast, some brain activity elicited by S_1 and S_{10} was not elicited by S_2 (e.g. frontal lobe activity in the timeframe of 130–60 ms, Table 1). Such a pattern is compatible with the involvement of neural refractoriness in the N1 adaptive pattern.

In this study, non-specific areas showed much stronger current densities in the S_1 response than in responses to other stimuli; Temporal lobe activation was observed in response to all stimuli. This may be because most non-specific generators need a longer time to recover than the temporal lobe generator. The S_2 response may reflect the combined effects of adaptation and refractoriness of all components, displaying a dramatic reduction in voxel number compared to the S_1 response. At asymptotic amplitude levels (i.e., the S_{10} response), the N1 was dominated by the generators in the temporal lobe within the early N1 latency ranges (70–100 ms and 100–130 ms); activation of parietal and frontal lobe was observed in the later N1 latency range (130–160 ms). Our observations are consistent with the conclusion made by Näätänen (1992): the N1 peak elicited by the first stimulus in a train is mainly due to non-specific N1 generators. The amplitude decrement across subsequent stimuli reflects both the absence of the non-specific generators and the refractoriness of the supratemporal generators.

In a review article, Näätänen and Picton described at least 6 N1 components: Component 1 is generated in a much wider region of the supratemporal plane than that occupied by the primary auditory cortex. It has a negative peak at 100 ms and is most obvious in the frontocentral region of the scalp. Component 2 is generated in the association cortex on the lateral side of the temporal parietal cortex. It has a positive wave at approximately 100 ms and a negative wave at 150 ms. This component is maximally recorded at the midtemporal electrodes. Component 3 is probably from the motor and premotor cortices under the influence of the reticular formation and the ventral lateral nucleus of the thalamus, which projects to the precentral gyrus, the superior, middle and inferior frontal gyri, and the supplementary motor area on the mesial surface of the frontal lobe (Näätänen & Picton, 1987; Näätänen, 1992; Sokolov et al., 2001). The waveform of this component shows a negative peak at about 100 ms and is maximal at vertex electrodes. This component has nonspecific feature and is related to the orienting response to novel stimuli. Component 4 is the mismatch negativity generated from the supratemporal plane and it reflects an automatic comparison between the present stimulus and the preceding stimuli. Component 5 is the sensory-specific processing negativity that starts at 50–100 ms and lasts during the processing of an attended stimulus. This component may be generated in the auditory cortex on the supratemporal plane and the areas on the lateral aspects of the temporal lobe. Component 6 is the second component of the processing negativity that may be generated in the anterior frontal cortex. Among the 6 components, the first 3 components were regarded as the “true” N1 components that contribute to auditory perception.

In the current study, the S_{10} response should be most comparable LAEP to that evoked by stimuli at a fixed and fast rate in most previous studies, due to the short ISI of 0.7 ms and the fact that the LAEP amplitude reaches an asymptote well before S_{10}. Table 1 and Figure 3 show that the temporal lobe was the dominant generator of the N1 for the earlier timeframes (70–100 ms and 100–130 ms), and that the frontal and parietal regions were recruited for the late timeframe of 130–160 ms. The generators observed for the S_{10} response may correspond to the first two “true” N1 components in Näätänen and Picton (1987) and an additional components in the nonspecific areas.

In contrast to the S_{10} response that is largely affected by neural adaptation and/or refractoriness, the S_1 response reflects activities that involve most N1-relevant generators least affected by neural adaptation and/or refractory process. This is because the long inter-train interval, ie., 15 seconds, allows for a full recovery of most generators. In the sLORETA results of the S_1 response, significantly increased activation was seen in non-specific regions in the frontal lobe, occipital lobe, parietal lobe, and limbic lobe. Therefore, the generators in the S_1 response may correspond to at least the first 3 components in Näätänen and Picton's study (1987).

In sum, the sLORETA results suggested that N1 generators can be roughly grouped into 3 components. The first is the obligatory N1 component in the auditory cortex and association areas which correspond to Näätänen and Picton's first two components (see temporal lobe activation in the early latency range of S_{10} response); the second is the obligatory N1 component in non-specific areas (see frontal and parietal activation in the late latency range of S_{10} response); the third is the orienting N1 component in non-specific areas (see brain activation in S_1 response). The first two components need a relatively short time to recover so that they can be seen in both S_{10} response and S_1 response (see the structures in the mildly shaded area in Table 1). The third component needs a long time to recover so that it can only be seen in S_1 response but not S_2 and S_{10} response (see the structures in the heavily shaded area in Table 1). Our categorization is supported by findings in ERP, fMRI, and intracerebral recordings (Anderer et al., 1998; Picton et al., 1999; Gallinat et al., 2002; Giard et al., 1994; Rosburg et al., 2005; Mayhew et al., 2010). The 130–160 ms activity in the fronto-parietal network was only seen in S_1 but not necessarily in S_1 and S_{10} responses while activity in the early latency ranges in the temporal lobes was elicited by all three stimuli. The current sLORETA results imply different recovery dynamics in the temporal and frontal lobes: a long recovery time for the frontal-parietal network and a relatively short recovery time for the supratemporal component.

Our categorization can unify some discrepancies in the literature. For instance, Alcaini et al. (1994) suggested that two more components in addition to Näätänen and Picton's 3 "true" N1 components also contribute to the N1: one is an obligatory frontal component that can be elicited whatever the stimulus rate and has a short recovery time, and the other is an auditory cortex component in response to infrequent stimuli that needs a long time to recover. In fact, Alcaini's two components can be grouped into the second and third components in our sLORETA categories.

3.3. Brain functions associated with the N1 adaptive pattern

The present study provided important information on the temporal dynamics of N1 adaptive pattern. The mean sLORETA difference map between S_1 and S_2 responses displayed activation in different regions within the different timeframes: the parietal lobe (inferior parietal lobule, postcentral gyrus) in the 70–100 ms timeframe, the limbic (cingulate gyrus) and frontal lobes (middle frontal gyrus, precentral gyrus) in the 100–130 ms timeframe, and the frontal lobe (inferior frontal gyrus, orbital gyrus) in the 130–160 ms timeframe. The results provide support for previous speculations that there may be an anterior-posterior brain network for novel stimulus detection (Baudena et al., 1995; Cycowicz & Friedman, 1997; Opitz et al., 2002; Rosburg et al., 2005). Previous studies reported that, when an infrequent stimulus occurs, a pre-attentive mechanism in the frontal lobe is activated (Cycowicz & Friedman, 1997; Opitz et al., 2002). If attention is involved, the attention-driven detection of stimulus is then transmitted to temporal-parietal areas (Polish, 1989; Friedman et al., 1998; Polich, 2007). The involvement of the parietal lobe may reflect the matching of sensory information to memory templates (Friedman et al., 1998; Knight & Nakada, 1998). In his study, the activation of the parietal and frontal lobes in the difference sLORETA map between S_1 and S_2 responses may suggest the hypothesis that the parieto-

frontal network enables the brain to filter out irrelevant and repeated stimuli. This network may serve to enhance the sensitivity of the auditory brain for incoming novel and significant stimuli.

3.4. Clinical implications and future studies

This study provides essential preliminary data for normal controls, setting the stage for further studies of abnormal adaptive pattern in individuals with relevant pathologies (e.g., CI users). For CI users, long term deafness may alter brain structures, as well as the adaptation/refractory features of neural responses. Electric stimulation by the implant would elicit brain plasticity (Guiraud et al., 2007). Zhang et al. (2010) reported that the LAEP waveform in poor CI performers exhibited less amplitude reduction compared with NH young listeners or good CI performers. It is possible that the N1 generators may be differentially compromised across CI patients, resulting in a large inter-subject variability in CI outcomes. CI patients cannot be tested with neuroimaging techniques such as the fMRI and MEG. Therefore, EEG and current density reconstruction may be valuable for diagnosing neurological and/or auditory impairment for individual CI patients. Such objective measures would be especially useful in pediatric or adult CI patients who cannot be behaviorally tested. These techniques would also allow for objective measures of brain plasticity associated with CIs.

3.5. Conclusions

The current study showed that brain activation for the N1 involved both auditory cortical areas in the temporal lobe and non-specific regions in other lobes. The contribution of non-specific regions was greater for the response evoked by the first stimulus than for the response evoked by later stimuli in the train, due to a more complete recovery of these generators over the long inter-train interval. There is a parieto-frontal brain network involved in the N1 adaptive pattern. This network may serve as a filter to remove excessive auditory information and thereby may help enhance the sensitivity of the auditory brain for novel and significantly stimuli.

4. Experimental procedures

4.1. Participants

Fourteen right-handed healthy human subjects (20–30 years, 13 females and 1 male) were recruited. All participants were normal hearing (pure tone air-conduction thresholds < 20 dB HL at octave frequencies from 0.5 to 4 kHz), normal type A tympanometry and normal acoustic reflex thresholds at 0.5, 1 and 2 kHz. They were free of psychiatric, neurologic and alcohol/drug abuse history. They were also free of medications and were required to abstain from alcohol, drugs, caffeine and nicotine prior to recordings. After providing written informed consent, each participant was fitted with a 40-channel Neuroscan quick-cap and was comfortably seated in a sound treated booth for electroencephalographic recordings. Participants were financially compensated for their time. The research protocol was approved by the Institutional Review Board of the University of Cincinnati.

4.2. Stimuli

The stimuli were 1 kHz tone bursts (60 ms, 10 ms rise/fall time) that were digitally generated and presented using Neuroscan's STIM^2 software and hardware (Compumedics Neuroscan, Inc., Charlotte, NC). The stimuli were presented in trains of 10 tone bursts, with an ISI of 0.7 s and an inter-train interval (ITI) of 15 s. This ITI allowed a nearly full recovery of the LAEP from adaptation and/or refractory time following the response to preceding stimuli. The presented stimuli in one recording included 30 trains of tone bursts.

At least two recordings were obtained from each participant. The stimuli were presented binaurally via ER-3A insert earphones at 80 dB SPL.

4.3. Electroencephalographic recording

The EEG recordings were performed using Neuroscan's 40-channel Nuamps system. The electrode cap was placed on the scalp based on the International 10–20 system, with the linked ears as the reference. Electroocular activity (EOG) was monitored so that eye movement artifacts could be identified and rejected during the offline analysis. Electrode impedances in all electrodes were kept at or below 5 kΩ. EEG recordings were collected from participants using Neuroscan's SCAN software (version 4.3) with a band-pass filter of 0.1 to 100 Hz and an analog-to-digit-converter (ADC) sampling rate of 1000 Hz. During the experiment, participants read self-chosen books to keep alert and were asked to ignore the acoustic stimuli. Participants were given short breaks in order to avoid fatigue and to maximize alertness.

4.4. Data Analysis

4.4.1. Waveform analysis—EEG data analysis was performed using EEGLAB 6.03, an online open source toolbox (Delorme & Makeig, 2004) running under Matlab 6.3 (The Mathworks, Natick, MA). Continuous EEG data were digitally filtered (0.3–30 Hz with a slope of 12/dB octave) and epoched between −100 to 500 ms. After rejecting approximately 10% of all epochs that contained excessive noise, the remaining data epochs were concatenated into a single-trial dataset for each subject. An average reference for each of the scalp electrodes was computed (Anderer et al., 1998). After baseline correction using the pre-stimulus window, EEG data were then decomposed using independent component analysis (ICA), which separates the EEG dataset into mutually independent components, including those from artifactual and neutral EEG sources (ICA, Delorme & Makeig, 2004; Jung et al., 2000). Components representing artifacts associated with blinks, additional eye movements, muscular artifacts were removed. Details of artifact removal using ICA are provided in our previous paper (Zhang et al., 2009b). After removing artifacts, the remaining components were then constructed to form the final EEG dataset and responses from the repeated recordings were combined. Then the combined EEG dataset was separately averaged to obtain one LAEP for each consecutive stimulus in the train. Thus, there were equal numbers of epochs for each stimulus in the train.

4.4.2. Source analysis using sLORETA—The sLORETA, an online available source analysis method (Pascual-Marqui, 2002), was performed on the LAEP data to localize neural generators for the N1 evoked by the first (S_1), second (S_2) and tenth stimuli (S_{10}). The data for the third through ninth stimuli (S_3–S_9) were not used for source analysis because previous work of waveform analysis showed no response difference in morphology, peak amplitude, and latency between S_3–S_9 and S_{10} (Zhang et al., 2009a). The voxel-based data were created according to the LAEP data from 34 electrodes (FP1, FP2, F7, F3, FZ, F4, F8, FT7, FC3, FCz, FC4, FT8, T3, C3, CZ, C4, T4, TP7, CP3, CPz, CP4, TP8, T5, P3, PZ, P4, T6, O1, OZ, O2, FT9, FT10, PO1, PO2) in 3 timeframes (70–100 ms, 100–130 ms and 130–160 ms) for S_1, S_2 and S_{10}. These three timeframes corresponded to the latency ranges of three main waveform subcomponents of the N1 and has been used to quantify the adaptive pattern of N1 waveform subcomponents (N1a, N1b, and N1c, Picton & Stuss, 1980; Näätänen & Picton, 1987; Woods, 1995; Budd et al., 1998). Activation within each timeframe was compared to the pre-stimulus period within each stimulus (Knott et al., 2009). The sLORETA results for the three timeframes were also compared across stimuli (i.e., S_1 vs. S_2 and S_2 vs. S_{10}. The comparison between S_1 vs. S_{10} was not performed because S_{10} and S_2 responses are similar).

4.4.3. Statistical analysis—The amplitude and latencies of the N1 derived from the LAEP waveforms were subjected to separate repeated measures analyses of variance (RM ANOVAs) to determine whether differences in responses evoked by S_1, S_2, and S_{10} were significant. Data from Cz were used since Cz has been reported to be associated with the largest N1 amplitude.

sLORETA Comparisons were performed for 1) within-stimulus comparisons between current source density (CSD) values within the timeframes of 70–100 ms, 100–130 ms and 130–160 ms and those within the pre-stimulus period, and 2) between-stimulus comparisons between CSD values within each timeframe of 70–100 ms, 100–130 ms, and 130–160 ms (i.e., S_1 vs.S_2, S_2 vs S_{10}). The within-stimulus comparisons were used to describe the CSD distribution of N1 evoked by S_1, S_2, and S_{10}. The between-stimulus comparisons provided information on the differences in CSD distribution for S_1, S_2, and S_{10}. Specifically, the obtained sLORETA images were compared between timeframes using the sLORETA-built-in voxel-wise randomization tests based on statistical non-parametric mapping (SnPM) corrected for multiple comparisons (Holmes et al. 1996). The voxels with significant differences were specified in the corresponding brain regions using sLORETA images and voxel-by-voxel t-values in Talairach space are displayed as statistical parametric maps (SPMs).

In order to provide a general, rather than detailed picture of brain activation, a conservative significance level ($p < 0.01$) was used for the within- and between-stimulus comparisons in the CSD values. For other data such as the waveform analysis, $p < 0.05$ was used.

Research Highlights

- Multiple brain regions contribute to the N1 of the late auditory evoked potential.
- The N1 displays amplitude adaptation following stimulus repetition.
- There is a parieto-frontal brain network involved in N1 adaptation.

Abbreviations

AEPs	Auditory evoked potentials
CI	Cochlear implant
EEG	Electroencephalography
EOG	Electrooculography
ICA	Independent component analysis
ISI	Inter-stimulus interval
ITI	Inter-train interval
LAEP	Late auditory evoked potential
NH	Normal hearing
sLORETA	standardized Low Resolution Electromagnetic Tomography

Acknowledgments

The authors thank all participants in this research. Special thanks to Dr. John J. Galvin III for editorial assistance. This project is partially sponsored by National Institute of Health (NIH 1R15DC011004-01).

REFERENCES

Alcaini M, Giard MH, Thevenet M, et al. Two separate frontal components in the N1 wave of the human auditory evoked response. Psychophysiology. 1994; 31:611–615. [PubMed: 7846222]

Anderer P, Pascual-Marqui RD, Semlitsch HV, Saletu B. Differential effects of normal aging on sources of standard N1, target N1 and target P300 auditory event-related brain potentials revealed by low resolution electromagnetic tomography (LORETA). Electroencephalogr Clin Neurophysiol. 1998; 108:160–174. [PubMed: 9566629]

Barry RJ, Cocker KI, Anderson JW, et al. Does the N100 evoked potential really habituate? Evidence from a paradigm appropriate to a clinical setting. Int J Psychophysiol. 1992; 13:9–16. [PubMed: 1522037]

Baudena P, Halgren E, Heit G, Clarke JM. Intracerebral potentials to rare target and distractor auditory and visual stimuli III frontal cortex. Electroencephalogr Clin Neurophysiol. 1995; 94:251–264. [PubMed: 7537197]

Bourbon WT, Will KW, Gary HE Jr, et al. Habituation of auditory event-related potentials: A comparison of self-initiated and automated stimulus trains. Electroencephalogr Clin Neurophysiol. 1987; 66:160–166. [PubMed: 2431880]

Budd TW, Barry RJ, Gordon E, et al. Decrement of the N1 auditory event-related potential with stimulus repetition: Habituation vs refractoriness. Int J Psychophysiol. 1998; 31:51–68. [PubMed: 9934621]

Cycowicz YM, Friedman D. A developmental study of the effect of temporal order on the ERPs elicited by novel environmental sounds. Electroencephalogr Clin Neurophysiol. 1997; 103:304–318. [PubMed: 9277633]

Delgutte, B. Auditory neural processing of speech. In: Hardcastle, WJ.; Laver, J., editors. The handbook of phonetic sciences. Oxford: Blackwell; 1997. p. 507-538.

Delorme A, Makeig S. EEGLAB: An open source toolbox for analysis of single-trial EEG dynamics including independent component analysis. J Neurosci Methods. 2004; 134:9–21. [PubMed: 15102499]

Eggermont JJ, Ponton CW. The neurophysiology of auditory perception: From single units to evoked potentials. Audiol Neurootol. 2002; 7:71–99. [PubMed: 12006736]

Fitzpatrick DC, Kuwada S, Kim DO, et al. Responses of neurons to click-pairs as simulated echoes: Auditory nerve to auditory cortex. J Acoust Soc Am. 1999; 106:3460–3472. [PubMed: 10615686]

Friedman D, Kazmerski VA, Cycowicz YM. Effects of aging on the novelty P3 during attend and ignore oddball tasks. Psychophysiology. 1998; 35:508–520. [PubMed: 9715095]

Fruhstorfer H. Habituation and dishabituation of the human vertex response. Electroencephalogr Clin Neurophysiol. 1971; 30:306–312. [PubMed: 4103502]

Gallinat J, Mulert C, Bajbouj M, et al. Frontal and temporal dysfunction of auditory stimulus processing in schizophrenia. NeuroImage. 2002; 17:110–127. [PubMed: 12482071]

Giard MH, Perrin F, Echallier JF, et al. Dissociation of temporal and frontal components in the human auditory N1 wave: A scalp current density and dipole model analysis. Electroencephalogr Clin Neurophysiol. 1994; 92:238–252. [PubMed: 7514993]

Grech R, Cassar T, Muscat J, Camilleri KP, Fabri SG, Zervakis M, et al. Review on solving the inverse problem in EEG source analysis. J Neuroeng Rehabil. 2008; 5:25. [PubMed: 18990257]

Groenen PA, Beynon AJ, Snik AF, et al. Speech-evoked cortical potentials and speech recognition in cochlear implant users. Scand Audiol. 2001; 30:31–40. [PubMed: 11330917]

Guiraud J, Besle J, Arnold L, et al. Evidence of a tonotopic organization of the auditory cortex in cochlear implant users. J Neurosci. 2007; 27:7838–7846. [PubMed: 17634377]

Hari R, Kaila K, Katila T, et al. Interstimulus interval dependence of the auditory vertex response and its magnetic counterpart: Implications for their neural generation. Electroencephalogr Clin Neurophysiol. 1982; 54:561–569. [PubMed: 6181979]

Hari R, Sams M, Jarvilehto T. Auditory evoked transient and sustained potentials in the human EEG: I effects of expectation of stimuli. Psychiatry Res. 1979; 1:297–306. [PubMed: 298357]

Hine J, Debener S. Late auditory evoked potentials asymmetry revisited. Clin Neurophysiol. 2007; 118:1274–1285. [PubMed: 17462945]

Holmes AP, Blair RC, Watson JD, Ford I. Nonparametric analysis of statistic images from functional mapping experiments. J Cereb Blood Flow Metab. 1996; 16:7–22. [PubMed: 8530558]

Järvilehto T, Hari R, Sams M. Effect of stimulus repetition on negative sustained potentials elicited by auditory and visual stimuli in the human EEG. Biol Psychol. 1978; 7:1–12. [PubMed: 747714]

Jung TP, Makeig S, Humphries C, et al. Removing electroencephalographic artifacts by blind source separation. Psychophysiology. 2000; 37:163–178. [PubMed: 10731767]

Knight RT, Scabini D, Woods DL, et al. The effects of lesions of superior temporal gyrus and inferior parietal lobe on temporal and vertex components of the human AEP. Electroencephalogr Clin Neurophysiol. 1988; 70:499–509. [PubMed: 2461284]

Knight RT, Nakada T. Cortico-limbic circuits and novelty: A review of EEG and blood flow data. Rev Neurosci. 1998; 9:57–70. [PubMed: 9683327]

Knott V, Millar A, Fisher D. Sensory gating and source analysis of the auditory P50 in low and high suppressors. NeuroImage. 2009; 44:992–1000. [PubMed: 19007892]

Kooi KA, Tipton AC, Marshall RE. Polarities and field configurations of the vertex components of the human auditory evoked response: A reinterpretation. Electroencephalogr Clin Neurophysiol. 1971; 31:166–169. [PubMed: 4104706]

Loquet G, Pelizzone M, Valentini G, et al. Matching the neural adaptation in the rat ventral cochlear nucleus produced by artificial (electric) and acoustic stimulation of the cochlea. Audiol Neurootol. 2004; 9:144–159. [PubMed: 15084819]

Lu ZL, Williamson SJ, Kaufman L. Human auditory primary and association cortex have differing lifetimes for activation traces. Brain Res. 1992; 572:236–241. [PubMed: 1611518]

Martin BA, Tremblay KL, Korczak P. Speech evoked potentials: From the laboratory to the clinic. Ear Hear. 2008; 29:285–313. [PubMed: 18453883]

Mayhew SD, Dirckx SG, Niazy RK, Iannetti GD, Wise RG. EEG signatures of auditory activity correlate with simultaneously recorded fMRI responses in humans. Neuroimage. 2010; 49:849–864. [PubMed: 19591945]

McEvoy L, Levanen S, Loveless N. Temporal characteristics of auditory sensory memory: Neuromagnetic evidence. Psychophysiology. 1997; 34:308–316. [PubMed: 9175445]

Näätänen R, Picton T. The N1 wave of the human electric and magnetic response to sound: A review and an analysis of the component structure. Psychophysiology. 1987; 24:375–425. [PubMed: 3615753]

Näätänen, R. Attention and Brain Function. Hillsdale, New Jersey: LEA; 1992.

Opitz B, Rinne T, Mecklinger A, et al. Differential contribution of frontal and temporal cortices to auditory change detection: FMRI and ERP results. NeuroImage. 2002; 15:167–174. [PubMed: 11771985]

Pascual-Marqui RD. Standardized low-resolution brain electromagnetic tomography (sLORETA). Technical details. Methods Find Exp Clin Pharmacol. 2002; 24 Suppl D:5–12.

Picton TW, Stuss DT. The component structure of the human event-related potentials. Prog Brain Res. 1980; 54:17–48. [PubMed: 7220911]

Picton TW, Alain C, Woods DL, et al. Intracerebral sources of human auditory-evoked potentials. Audiol Neurootol. 1999; 4:64–79. [PubMed: 9892757]

Polich J. Updating P300: An integrative theory of P3a and P3b. Clin Neurophysiol. 2007; 118:2128–2148. [PubMed: 17573239]

Ponton CW, Don M, Eggermont JJ, et al. Maturation of human cortical auditory function: Differences between normal-hearing children and children with cochlear implants. Ear Hear. 1996; 17:430–437. [PubMed: 8909891]

Pool KD, Finitzo T, Hong CT, et al. Infarction of the superior temporal gyrus: A description of auditory evoked potential latency and amplitude topology. Ear Hear. 1989; 10:144–152. [PubMed: 2744249]

Prosser S, Arslan E, Michelini S. Habituation and rate effect in the auditory cortical potentials evoked by trains of stimuli. Arch Otorhinolaryngol. 1981; 233:179–187. [PubMed: 7316876]

Ritter W, Vaughan HG Jr, Costa LD. Orienting and habituation to auditory stimuli: A study of short term changes in average evoked responses. Electroencephalogr Clin Neurophysiol. 1968; 25:550–556. [PubMed: 4178749]

Rosburg T, Trautner P, Dietl T, Korzyukov OA, Boutros NN, Schaller C, et al. Subdural recordings of the mismatch negativity (MMN) in patients with focal epilepsy. Brain. 2005; 128:819–828. [PubMed: 15728656]

Scherg M, Von Cramon D. Two bilateral sources of the late AEP as identified by a spatio-temporal dipole model. Electroencephalogr Clin Neurophysiol. 1985; 62:32–44. [PubMed: 2578376]

Shore SE. Recovery of forward-masked responses in ventral cochlear nucleus neurons. Hear Res. 1995; 82:31–43. [PubMed: 7744711]

Squires NK, Squires KC, Hillyard SA. Two varieties of long-latency positive waves evoked by unpredictable auditory stimuli in man. Electroencephalogr Clin Neurophysiol. 1975; 38:387–401. [PubMed: 46819]

Sokolov EN, Nezlina NI, Polianskii VB, Evtikhin DV. Orienting reflex: "targeting reaction" and "searchlight of attention.". Neurosci Behav Physiol. 2001; 32:347–362. [PubMed: 12243255]

Thompson RF, Spencer WA. Habituation: a model phenomenon for the study of neuronal substrates of behavior. Psychol Rev. 1966; 73:16–43. [PubMed: 5324565]

Vaughan HG Jr, Ritter W. The sources of auditory evoked responses recorded from the human scalp. Electroencephalogr Clin Neurophysiol. 1970; 28:360–367. [PubMed: 4191187]

Wagner M, Fuchs M, Kastner J. Evaluation of sLORETA in the presence of noise and multiple sources. Brain Topogr. 2004; 16:277–280. [PubMed: 15379227]

Westerman LA, Smith RL. Rapid and short-term adaptation in auditory nerve responses. Hear Res. 1984; 15:249–260. [PubMed: 6501113]

Woods DL. The component structure of the N1 wave of the human auditory evoked potential. Electroencephalogr Clin NeurophysiolSupplement. 1995; 44:102–109.

Woods DL, Clayworth CC, Knight RT, et al. Generators of middle- and long-latency auditory evoked potentials: Implications from studies of patients with bitemporal lesions. Electroencephalogr Clin Neurophysiol. 1987; 68:132–148. [PubMed: 2435529]

Woods DL, Elmasian R. The habituation of event-related potentials to speech sounds and tones. Electroencephalogr Clin Neurophysiol. 1986; 65:447–459. [PubMed: 2429824]

Zhang F, Eliassen E, Anderson JM, et al. Time course of the late latency auditory evoked response to repeated stimuli. J Am Acad Audiol. 2009a; 20:239–250. [PubMed: 19927696]

Zhang F, Samy R, Anderson JM, Houston L. The recovery function of the late auditory evoked potential in CI users and normal listeners. J Am Acad Audiol. 2009b; 20:397–408. [PubMed: 19928394]

Zhang F, Anderson J, Samy R, Houston L. The adaptive pattern of the late auditory evoked potential elicited by repeated stimuli in cochlear implant users. Int J Audiol. 2010; 49:277–285. [PubMed: 20151878]

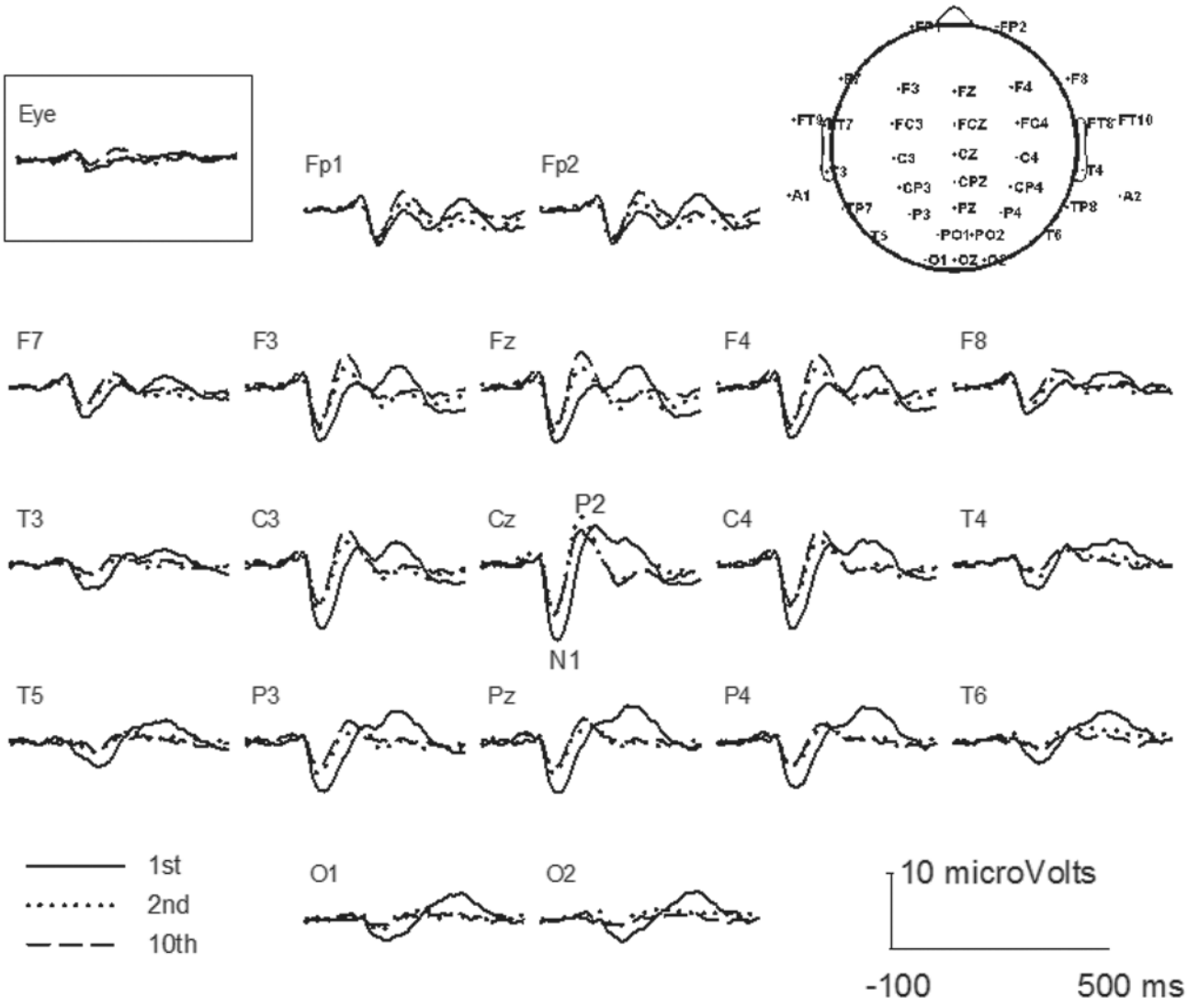

Fig. 1.

Grand mean for the LAEP at selected electrodes for the S_1, S_2 and S_{10} stimuli. The topographic map for 40-channel electrodes is shown at upper right.

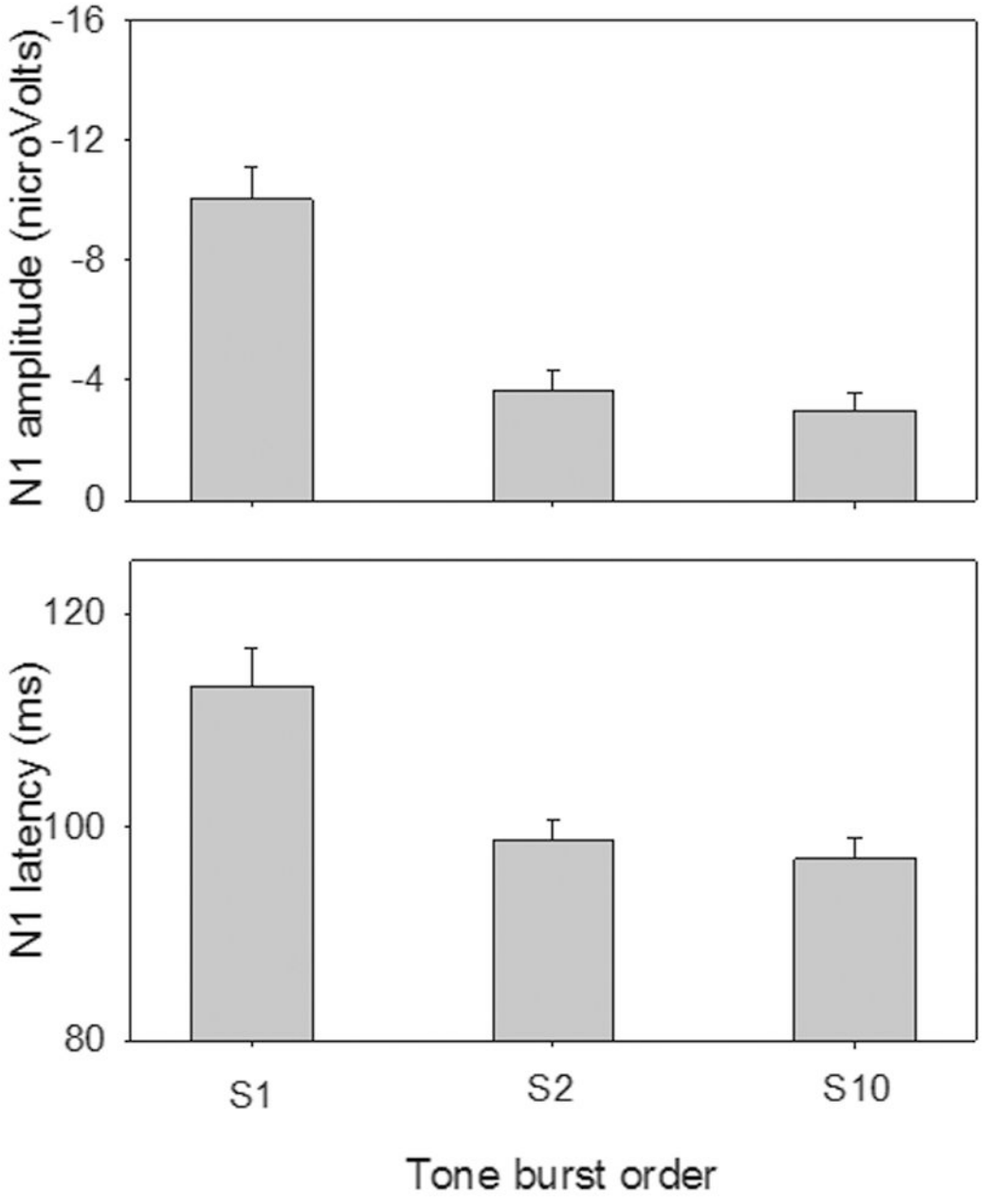

Fig. 2.
Mean amplitude and latency (across subjects) of the N1 for S_1, S_2, and S_{10} at electrode Cz. The error bars show 1 standard error of the mean.

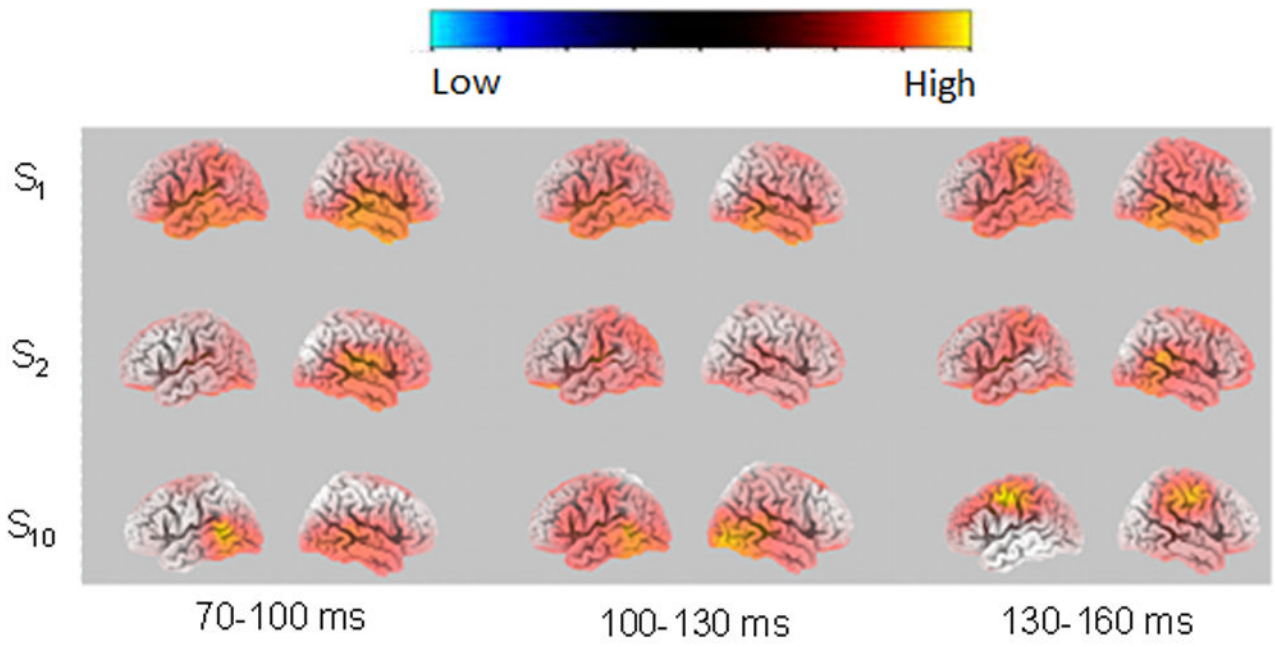

Fig. 3.

Left and right sLORETA statistical image (voxel-by-voxel *t*-tests) at the N1 time point corresponding to the maximum sLORETA value for the 70–100 ms, 100–130 ms and 130–160 ms timeframes, for S_1, S_2 and S_{10} (vs. baseline). The statistical images were derived by voxel-by-voxel *t*-tests.

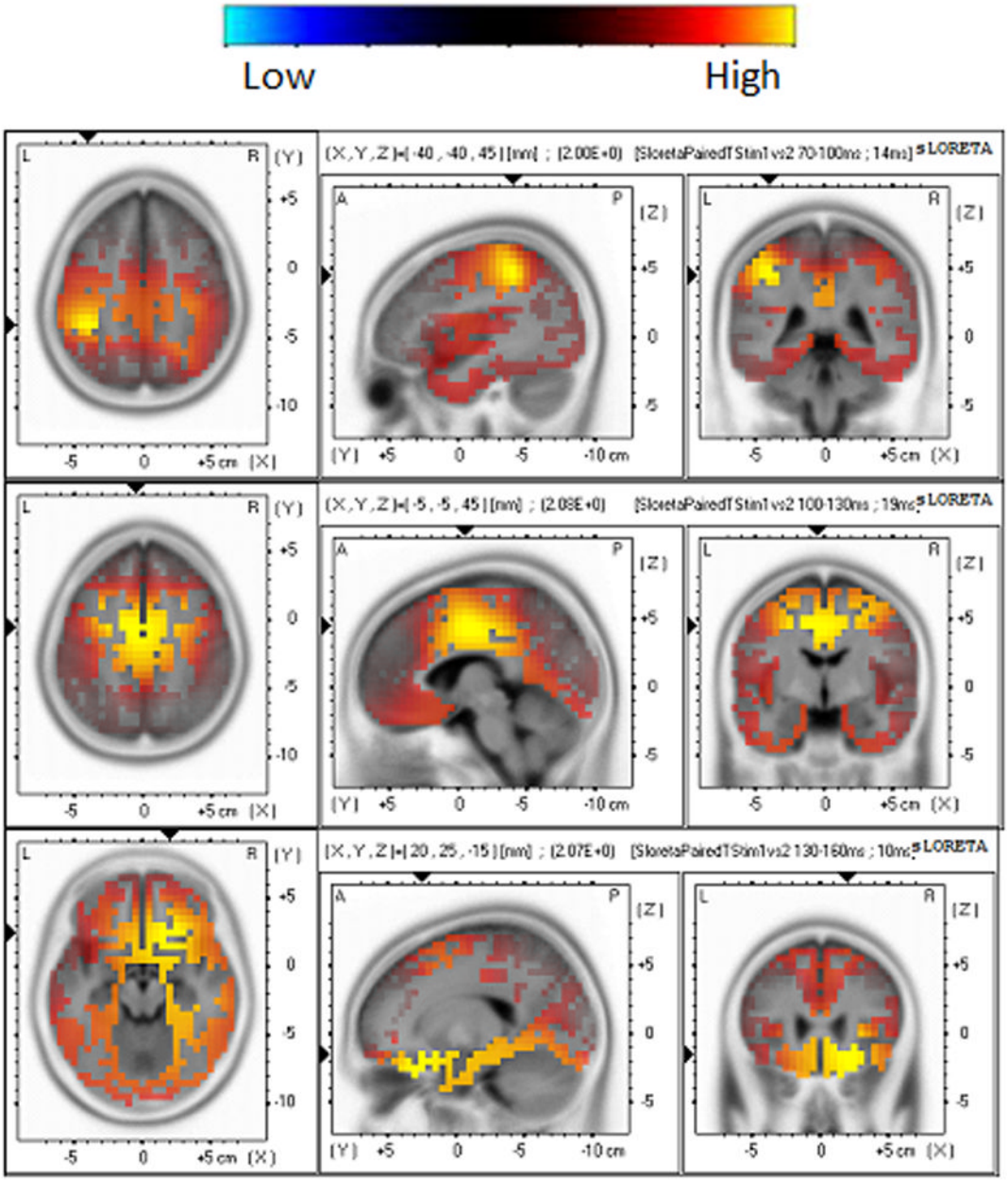

Fig. 4.

Horizontal, sagital and coronal slices of sLORETA statistical images (voxel-by-voxel *t*-tests, $p < 0.01$) derived from the difference between the S_1 and S_2 responses. The images are illustrated at time points of 94, 119, and 140 ms, i.e., the latencies corresponding to the maximum sLORETA for the 70–100 ms, 100–130 ms and 130–160 ms timeframes, respectively.

Table 1

sLORETA activations in response to the three stimuli at the time point corresponding to the maximum sLORETA values within each timeframe. Voxel number indicates the number of activated voxels. Each 'X' indicates significant activation ($p < 0.01$). The BA (Brodmann area) is also shown. The mildly shaded area includes structures that are categorized into Component 1 and 2 of the N1 peak; the heavily shaded area includes structures that are categorized into Component 3.

Timeframe		**70–100 ms**			**100–130 ms**			**130–160 ms**		
Stimulus number		**S_1**	**S_2**	**S_{10}**	**S_1**	**S_2**	**S_{10}**	**S_1**	**S_2**	**S_{10}**
Voxel number		**2816**	**378**	**94**	**1727**	**191**	**14**	**1651**	**64**	**581**
Brain region	BA area									
Limbic lobe										
Anterior Cingulate	32, 25	X	X		X	X		X		
Cingulate Gyrus	23, 24	X	X		X			X		
Parahippocampal Gyrus	36, 19	X	X		X	X		X	X	
Posterior Cingulate	30	X	X		X					
Uncus	28, 20	X	X		X	X		X		
Temporal lobe										
Fusiform Gyrus	20, 37	X	X	X	X			X		
Inferior Temporal Gyrus	20	X			X		X	X		
Middle Temporal Gyrus	22	X		X	X			X		
Sub-Gyral	20, 21	X			X			X		
Superior Temporal Gyrus	22, 38	X	X	X	X	X		X		X
Transverse Temporal Gyrus	41, 42	X	X		X	X		X		X
Frontal Lobe										
Inferior Frontal Gyrus	47	X			X	X		X		X
Medial Frontal Gyrus	25	X	X		X	X		X		
Middle Frontal Gyrus	11	X			X			X		X
Orbital Gyrus	47, 11	X			X			X		
Precentral Gyrus	44	X	X		X			X		X
Rectal Gyrus	11	X	X		X	X		X		
Subcallosal Gyrus	25	X	X		X	X		X		

Timeframe		70–100 ms			100–130 ms			130–160 ms		
Stimulus number		S_1	S_2	S_{10}	S_1	S_2	S_{10}	S_1	S_2	S_{10}
Voxel number		**2816**	**378**	**94**	**1727**	**191**	**14**	**1651**	**64**	**581**
Superior Frontal Gyrus	11	X								
Occipital Lobe										
Fusiform Gyrus	19	X			X			X		
Inferior Occipital Gyrus	18	X			X					
Lingual Gyrus	18, 19	X			X					
Middle Occipital Gyrus	18, 19	X			X					
Parietal lobe										
Inferior Parietal Lobule	40	X						X		X
Postcentral Gyrus	3, 2	X	X		X			X		X
Sub-lobar										
Extra-Nuclear	13	X			X			X		
Insula	13	X	X		X	X		X		X

Table 2

The activated brain regions for each timeframe at $p < 0.01$ level for the difference map between S_1 and S_2.

Timeframe	Most activated lobe	Second-most activated lobe	t values for $p < 0.01$
70–100 ms	Parietal (inferior parietal lobule, postcentral gyrus)		1.867
100–130 ms	Frontal (middle frontal gyrus, precentral gyrus)	Limbic l (cingulate gyrus)	1.975
130–160 ms	Frontal (inferior frontal gyrus, orbital gyrus)		2.013